Int. J. Electrochem. Sci., 15 **(2020)** 5982 – 6000, doi: 10.20964/2020.07.62

International Journal of
ELECTROCHEMICAL
SCIENCE
www.electrochemsci.org

Corrosion Inhibition of α-brass Alloy in Aqueous Solution by Using Expired Ranitidine

A.S. Fouda[1,], S. Rashwaan[2], H. Ibrahim[2] and R.E. Ahmed[1]*

[1] Department of Chemistry, Faculty of Science, El-Mansoura University, El-Mansoura-35516, Egypt
[2] Department of Chemistry, Faculty of Science, Suez Canal University. Egypt.
[*]E-mail: asfouda@mans.edu.eg

Received: 2 March 2020 / *Accepted:* 24 April 2020 / *Published:* 10 June 2020

Expired Ranitidine was tested as a corrosion hindrance for α-brass**.** The result is utilized to identify its maximum concentration in order to be used in the protection of corrosion of α-brass in a HCl medium. The inhibitive action of Ranitidine is determined using mass loss (ML), potentiodynamic polarization (PP), electrochemical impedance spectroscopy (EIS) and electrochemical frequency modulation (EFM) tests. The efficiency of this Ranitidine depends on both concentration and temperature. The values of Gibbs free energy (ΔG^{o}_{ads}) (39 kJ mol^{-1}) indicated that *ER* is adsorbed on α-brass surface physico-chemically. The results indicate that Ranitidine exhibits excellent corrosion inhibition at 300 ppm and the inhibition effectiveness reached to 90%. The polarization data indicated that the tested Ranitidine affects both cathodic and anodic reactions (mixed kind). The Ranitidine is adsorbing on α-brass surface following Langmuir adsorption isotherm. The surface morphology of α-brass samples is analyzed.

Keywords: Acidic inhibition, α-brass, Ranitidine, EFM, EIS, AFM, FT.IR, SEM, EDX

1. INTRODUCTION

Brass is an alloy of zinc and copper with buttery yellow color, which has been make for thousands of years in numerous pieces of the world. α-brass is extensively utilized in industry due to good thermal and electrical conductivity and is often utilized in warming and cooling framework [1-9]. α-brass is disposed to a corrosion procedure identified as dezincification and this affinity improves with raising zinc content of the brass [10-11].

An enormous number of scientific investigations have been dedicated to the subject of corrosion protection for α-brass in acidic environment [12-23]**.** The Ranitidine drug has the following advantages: low toxicity and irritancy and it can be used orally and parentally controlled preparations, a greater degree of compatibility (with salts and all other), less sensitive to change in pH and electrolytes. Several authors have used drugs as corrosion inhibitors for α-brass in HCl solution [24-31]. The utilization of

pharmaceutical composite offers attractive chances for corrosion restraint because of the attendance of heteroatoms like nitrogen, sulfur and oxygen in their structure, and they are interest due to their protected use, high solvency in water and large atomic size. [32-34]. Also, the utilized of piperazine drug as a corrosion protection has been described [35]. Because, corrosion is significant topic in industry and academic research [36] many researchers concentrate their researches on this field.

In the present work, new expired drug (Ranitidine) was use as corrosion inhibitor for (α-brass) in 1M HCl solution as a corrosive medium by different chemical and electrochemical techniques.

2. EXPERIMENTAL METHODS

2.1. Materials and Solutions

The α-brass sample with the following conformation (weight%): 70% Cu and Zn 30 %. Test materials were abraded with various emery papers up to 1200 grade, washed with acetone, washed with double distilled water and appropriately dried prior to exposure. The aggressive solution 1 M HCl is prepared from 37% HCl (BDH grade). Ranitidine gotten from pharmaceutical company and was utilize for the study. The structure of Ranitidine is display in Fig. (1)

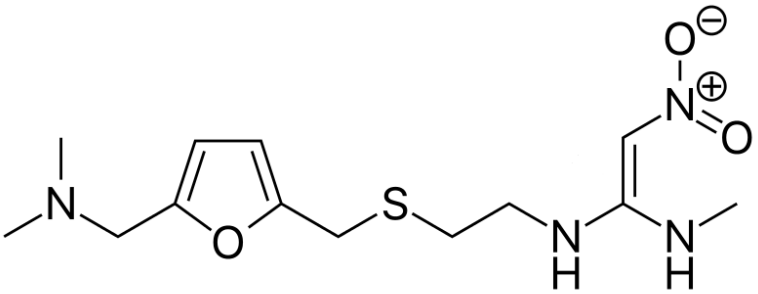

Figure 1. Molecular structure of Ranitidine drug

2.2. Mass loss (ML) test

(ML) is a method in which five pieces of metals with a dimension of 2cm×2cm are abraded well by emery papers that started with 300 and ended with 1200 grit size, then are weighed accurately and are put into 100 ml beaker containing 1M HCl with different concentrations of Ranitidine for 3 hours in water thermostat at 298 K. The (ML) is calculated per surface area and the inhibition percentage (IE%) is calculated by following equation [37].

$$\Delta W = (w_1 - w_2)/a \quad (1)$$

where the mass of the α-brass w_1 and w_2 before and after reaction, respectively, and the surface area (a).

$$IE\ \% = \theta \times 100 = [1 - (W / W°)] \times 100 \quad (2)$$

Where W° and W are the data of the average ML without and with Ranitidine, respectively

2.3. Electrochemical Measurements

2.3.1 Potentiodynamic Polarization Measurements

Three electrodes (Saturated calomel, Platinum electrode, and α-brass as working electrode (WE)) are put in the tested electrolytic solution until having a steady state (about 30 min). The (PP**)** tests is carried out at potential ranged from - 600 to + 400 mV vs. open circuit potential (E_{ocp}). The potential of an electrochemical solution was producing and measured the corrosion potential (E_{corr}) is measured and calculated the corrosion current from the slope of Tafel curve (i^{o}_{corr}) is calculated by Eq. (3)

$$\%IE= \theta \times 100= [1-(i_{corr}/i^{\circ}_{corr})] \times 100 \quad (3)$$

where i°_{corr} and i_{corr} are current densities without and with Ranitidine inhibitor, individually.

2.3.2. Electrochemical Impedance Spectroscopy (EIS) Measurements

The EIS technique is carried out at frequency range (100 kHz to 0.1 mHz) and 5 mV of the amplitude of peak.

2.3.3. Electrochemical Frequency Modulation (EFM) Measurements

EFM, study of these current responses due to Tafel parameters and corrosion current density [38-40]. The higher peaks were utilized to measure the (i_{corr}), (β_c and β_a) and the causality factors CF-2 and CF-3 [41].

In All electrochemical tests the WE are left in the test solution for around 30 min to reach a stable state of (OCP). Measurements had achieved utilizing Gamry Instrument Potentiostat/ Galvanostat/ ZRA (PCI4-G750). This consist of a Gamry framework system v 6.03 Gamry applications along with a computer for accumulating data.

2.4 Surface Analysis

Surface morphology of α-brass was investigated using Fourier transform spectroscopy (FTIR), atomic force microscopy (AFM) and scanning Electron Microscopy Measurements (SEM, EDX). After dipping in 1M HCl attendance and lack of the Ranitidine for 24 h at 25^{0}C. The α-brass clean with distilled water, dried and used to measure morphology of the surface.

2.5 Quantum Chemical Calculations

The molecular structures of the examined Ranitidine had adjusted initially with PM3 semi empirical test. All the quantum calculations had achieved with Material studio V. 6.0.

3. RESULTS AND DISCUSSION

3.1. ML measurements

ML tests were carried out using α-brass in 1 M HCl in the without and with of various concentrations of Ranitidine and are presented in Fig. (2). The (IE %) data are listed in Tables (1,2). From these tables, it is distinguished that the %IE improve with improving the concentration of Ranitidine and lowered with temperature increasing from 25-45ºC.

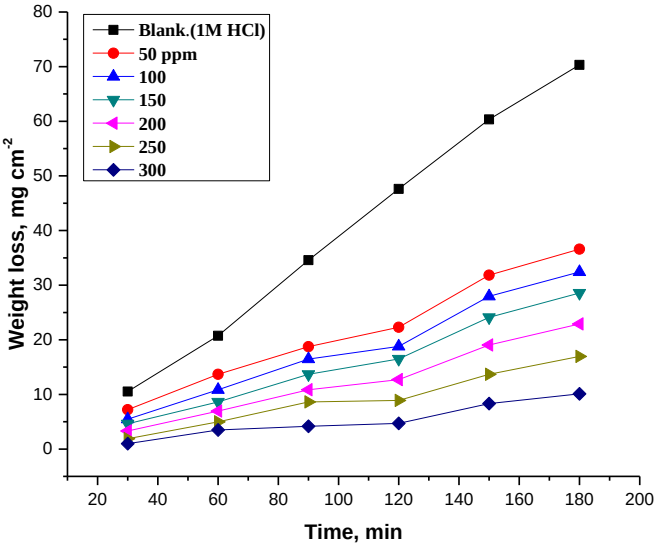

Figure 2. Time-ML bends for the corrosion of α-brass without and with various concentrations of Ranitidine at 298K

Table 1. The efficiency percentage (%IE) and (θ) of Ranitidine in 1 M HCl at 298 K

Conc., ppm	Corrosion rate ($\mathbf{k_{corr}}$) mg cm^{-2} min^{-1}	θ	%IE
Blank	0.23	--	--
50	0.10	0.552	55.2
100	0.08	0.621	62.1
150	0.06	0.693	69.3
200	0.05	0.758	75.8
250	0.03	0.841	84.1
300	0.02	0.924	92.4

3.2 Influence of Temperature

As the temperature improve, the corrosion rate ($\mathbf{k_{corr}}$) rises and the %IE of the drug lowered as presented in Table (2). The adsorption performance of drug on HCl surface happens through physical adsorption.

Table 2. %IE and (**k_{corr}**) of Ranitidine for the dissolution of α-brass in 1 M HCl at various concentrations and temperatures of 30-45˚C

[ER] x 10^6M	**30**˚C		**35**˚C		**40**˚C		**45**˚C	
	k_{corr}	**%IE**	**k_{corr}**	**%IE**	**k_{corr}**	**%IE**	**k_{corr}**	**%IE**
Blank	0.40	---	0.43	---	0.61	---	0.92	---
50	0.19	51.3	0.22	48.7	0.34	44.3	0.53	42.7
100	0.16	60.5	0.19	56.2	0.29	52.4	0.47	50.3
150	0.14	65.4	0.16	62.9	0.25	60.1	0.39	58.1
200	0.11	73.3	0.13	70.4	0.20	68.2	0.33	65.4
250	0.07	81.3	0.10	78.2	0.15	76.2	0.26	73.2
300	0.04	90.1	0.06	87.3	0.10	86.0	0.18	82.5

3.3. Adsorption Isotherm

Langmuir isotherm was applied which was found the best fitted isotherm. The next balance is the simplest form of the equation of Langmuir [42-45]:

$$C/\Theta) = 1/K_{ads} + C \quad (4)$$

Where C is the concentration of ER (mol./L), K_{ads} is constant of the adsorption equilibrium. Fig. (3) display the relation between $\frac{C}{\theta}$ vs. C which give straight lines at 20 °C for Ranitidine at various temperatures. These straight lines have slopes approximately equal unity and correlation coefficient $R^2 > 0.96$, this designates that the adsorption of Ranitidine obeys the Langmuir isotherm. Also, the standard free energy of adsorption (ΔG^o_{ads}) can be measured through this equation [46]:

$$K_{ads}=1/55.5 \exp [-\Delta G°_{ads}] / RT] \quad (5)$$

Where (R) is the gas constant is (8.314 J/ (mol. K)). However, the Table (3) the values of (K_{ads}) and (ΔG^o_{ads}) for inhibitor Ranitidine were listed. It is indicated from the values of the ΔG^o_{ads} that the adsorption of inhibitors includes both physisorption and chemisorption processes as the calculated values of -40 kJ/mol $< \Delta G_{ads}{}^o > -20$ kJ/mol [47]. Table (3) displayed that the adsorption of the Ranitidine is mixed form with both physisorption and chemisorption feature. In general, the higher K_{ads} and (ΔG^o_{ads}) values, the larger the capacity of compounds to adsorb and hence the greater inhibition effect.

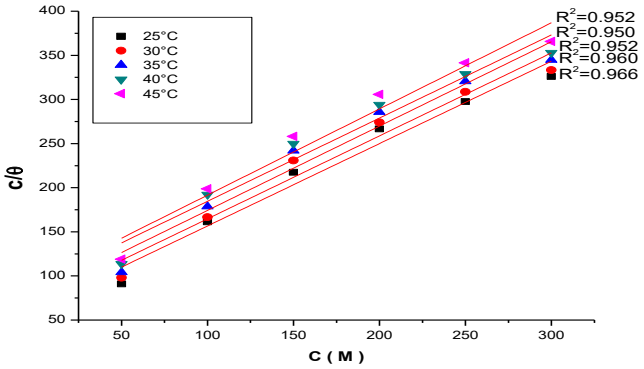

Figure 3. Langmuir diagrams for brass in 1 M HCl including various concentrations of Ranitidine at 298K

According to the Van's Hoff equation [48]. Plot of (ΔG^{o}_{ads}) against T. Fig. (4) give (ΔH^{o}_{ads}) and the entropy (ΔS^{o}_{ads}) from next equation 6:

$$\Delta G^{\circ}_{ads} = \Delta H^{\circ}_{ads} - T\Delta S^{\circ}_{ads} \quad (6)$$

The negative value of ΔG^{o}_{ads} reveals that the adsorption of Ranitidine on α-brass surface is spontaneous process [49] and the drug adsorbed on α-brass surface mainly physically. The values of ΔS°_{ads} in the existence of Ranitidine is great and negative that accompanied with exothermic adsorption procedure. This designates that an increase in disorder occurred on going from reactants to the α-brass adsorbed complex [50].

Table 3. The data of adsorption isotherm of Ranitidine at 25-45°C

Temp., °C	**Slope**	**K $_{ads}$x10^{-3} M^{-1}**	**-ΔG$^{o}_{ads}$ kJ mol^{-1}**	**-ΔH$^{o}_{ads}$ kJ mol^{-1}**	**-ΔS$^{o}_{ads}$ J mol^{-1} K^{-1}**
25	0.9638	15.90	39.2	16.5	77.62
30	0.9903	14.14	39.8		77.56
35	0.9882	12.71	40.4		77.56
40	0.9600	11.07	40.6		77.27
45	0.9770	10.65	41.2		77.77

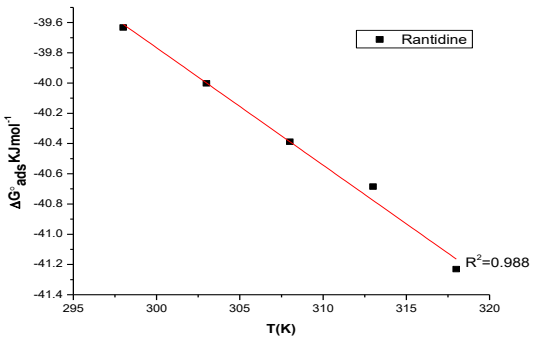

Figure 4. Difference of ΔG^{o}_{ads} vs. T for the drug adsorbed on α-brass

3.4 Kinetic –thermodynamic parameters

The influence of temperature on both corrosion and corrosion hindrance of α-brass in aggressive medium in the attendance and nonattendance of various concentration of drug at various temperatures ranging from 25ºC to 45ºC was deliberate utilizing ML. The rate of corrosion improves with raising temperature both in unprotected and protected acid. The parameters of activation for dissolution procedure measured from Arrhenius plot as below:

$$k_{corr} = A \exp^{(E^*a/RT)} \quad (7)$$

E^*_a can be gotten from the slope of log (k_{corr}) against 1/T plots lack and attendance of various concentrations of the Ranitidine as presented in Fig. (5). Data of E^*_a are reported in Table (4) Examination of the data displayed that E^*_a has greater data in attendance of the Ranitidine than that in its nonexistence. This has attributed the physical adsorption of Ranitidine on brass surface [51]. The transition state theory was used to compute the (ΔS^*) and (ΔH^*). The change data of (ΔS^*) and (ΔH^*) can be calculate by using the formula:

$$k_{corr} = (RT/Nh) \exp(^{\Delta S^*/R)} \exp^{(-\Delta H^*/RT)} \quad (8)$$

where k_{corr} the rate of metal dissolution. Fig. (6), demonstration a plan of log (k_{corr}/T) vs. (1/T) in the case of Ranitidine in 1 M HCl. The increase in E_a^* with raised Ranitidine concentration Table (4) is representative of physical adsorption. The value of ΔH^* had positive signs replicate the endothermic nature of the brass corrosion process [52] However, the value of (ΔS^*) decreases gradually with improving ER concentrations in the entire acid environment.

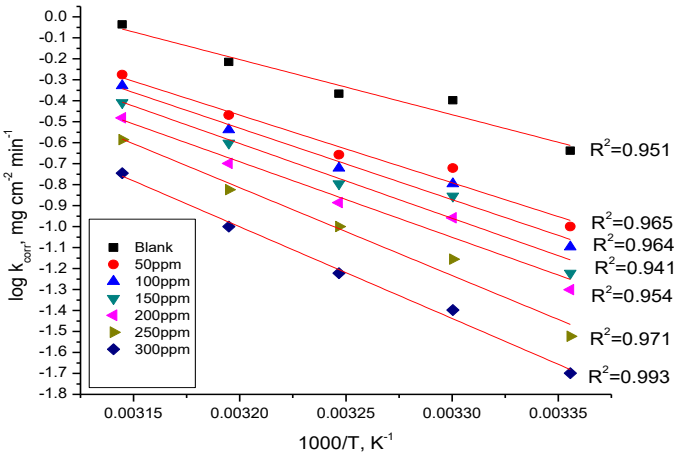

Figure 5. Log k_{corr} vs (1/T) plot for α-brass with and without various Ranitidine concentrations

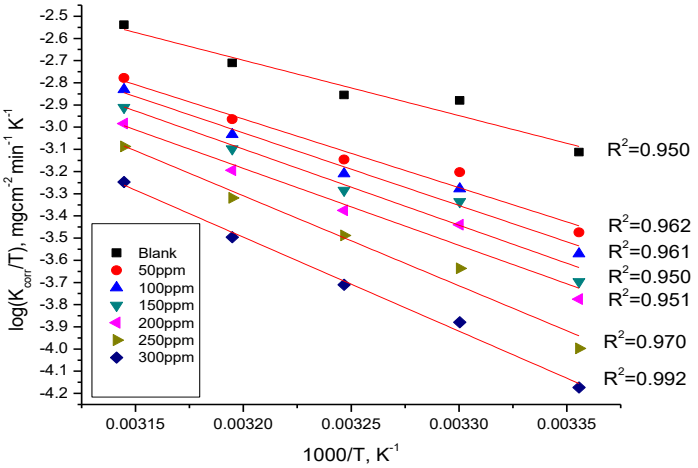

Figure 6. Log (k_{corr}/T) vs. (1/T) diagrams of dipping in 1M HCl in the absence and presence of various Ranitidine concentrations.

Table 4. Activation parameters for α-brass corrosion with and without various Ranitidine concentrations in 1M HCl

[inh] ppm	**A**	**E_a^* kJ mol^{-1}**	**ΔH^* kJ mol^{-1}**	**$-\Delta S^*$ J mol^{-1} K^{-1}**
0	0.23	50.8	47.8	105.5
50	2.03	61.7	59.2	93.2
100	2.11	65.2	62.6	89.9
150	3.14	68.2	65.8	83.4
200	10.96	69.3	66.5	75.6
250	68.23	80.2	76.6	71.4
300	396.2	83.7	81.1	68.9

3.5. Polarization measurements (PP)

Figure 7 demonstration PP bends registered for α-brass in 1 M HCl solutions non-utilize and utilize of various concentrations of Ranitidine at 298K. With the increment of the concentration of ER diagrams shifts both anodic and cathodic sections to the lesser data of i_{corr}, which lead to lowering in the corrosion rate. The PP bends had documented in Table (5), as the variation of the data of (log i_{corr}) with the (E_{corr}), (β_a, β_c), (**k_{corr}**), (θ) and (%IE). This means that Ranitidine retards both cathodic and anodic reactions of α-brass in aggressive medium. The slopes of anodic and cathodic Tafel lines (β_a and β_c), were lightly varied with the increasing the concentration of inhibitor. This designates that ER inhibitor signifies as mixed-type inhibitors [53-54].

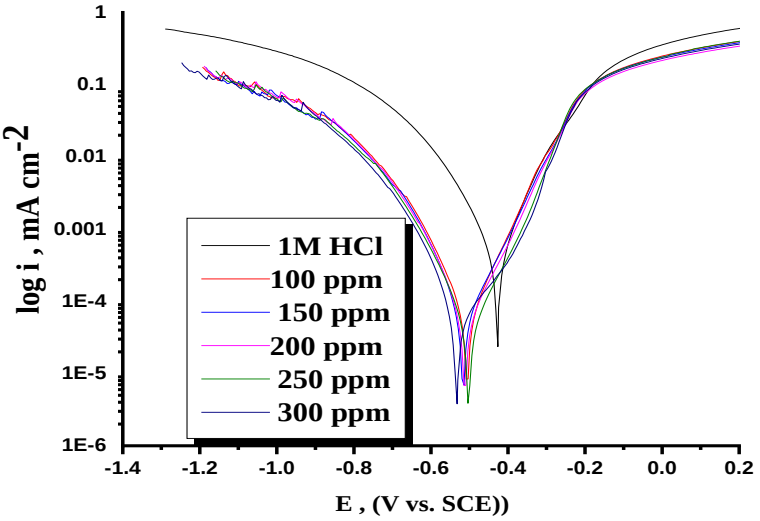

Figure 7. PP bends for the liquefaction of α-brass in 1M HCl with and without various concentrations of Ranitidine at 298K

Table 5. PP parameters of α-brass in 1M HCl at 298K for Ranitidine

[ER] (ppm)	i_{corr} mA/cm^2	$-E_{corr}$ (mV vs. SCE)	β_a mV/decade	β_c mV/decade	k_{corr}	% IE
blank	411	549	89	128	187.1	-
50	101	506	105	144	46.1	62
100	89.7	516	109	146	40.9	76
150	66.7	511	102	119	30.5	80
250	51.1	502	97	125	23.3	86
400	40.7	462	81	115	18.5	90

3.6 Electrochemical impedance spectroscopy (EIS)tests

EIS is well-established and it is great testing for corrosion study [55,59]. Fig. (8 a,b) represents the Nyquist and Bode diagrams. Fig.8a shows the semi-circle diameter was raised by increasing of Ranitidine concentration. Fig. (9), indicates the utilizing circuit for fitting the obtained results [60-61]. The C_{dl} and Y_0 were find from eq. (9) [62]:

$$C_{dl} = Y_0(\omega_{max})^{n-1} \quad (9)$$

where $\omega = 2\pi f_{max}$, f_{max} is the greater frequency and n is the exponential. R_{ct} improve with the rise of the double layer thickness [63]. From Table (6), the C_{dl} lowered as a result of the replacement of adsorbed water molecules by Ranitidine species [64-65].

The lower in CPE/C_{dl} results from a lower in local dielectric constant and/or an improve in the thickness of the double layer, signifying that Ranitidine protect the dissolution of brass by adsorption at brass/acid [66-67]. The %IE was measured from eq.10 [68]:

$$\% IE_{EIS} = [1 - (R^{\circ}_{ct}/ R_{ct})] \times 100 \quad (10)$$

where R_{ct} and R^{o}_{ct} are the charge-transfer resistance with and without Ranitidine, respectively.

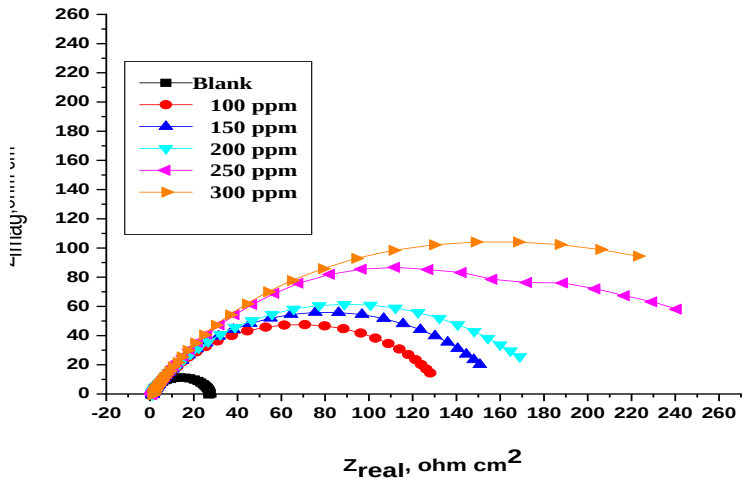

Figure 8a. EIS Nyquist plots of α-brass in 1M HCl with and without various concentrations of Ranitidine at 298K

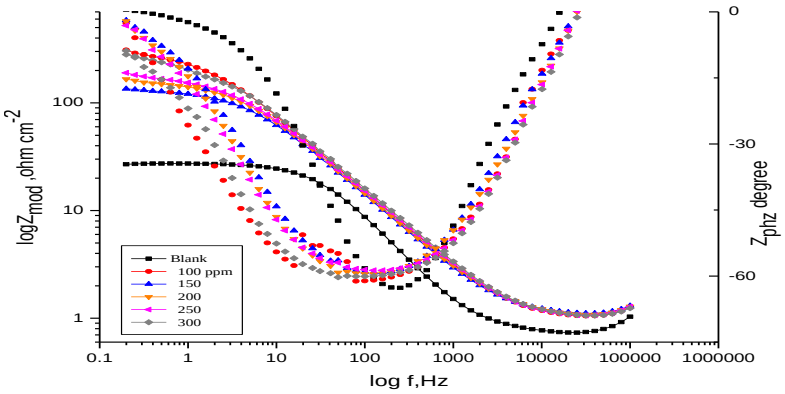

Figure 8b. EIS Bode plots of α-brass with and without various concentrations of Ranitidine at 298K

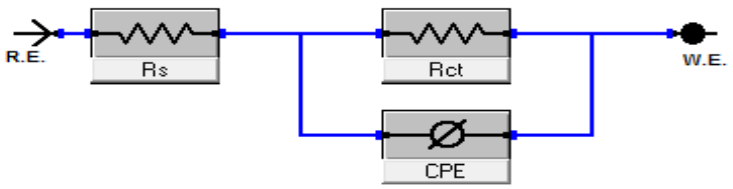

Figure 9. Circuit utilized for fitting the EIS data in 1M HCl

Table 6. EIS parameters for the dissolution of α-brass with and without various concentrations of Ranitidine at 298K

Conc., ppm	R_{ct} Ω cm^2	C_{dl} μF cm^{-2}	θ	% IE
Blank	30.5	300	--	--
100	98.6	237	0.702	70.2
150	119.2	215	0.754	75.4
200	178.3	155	0.804	80.4
250	212.2	150	0.858	85.8
300	333.1	130	0.918	91.8

3.7. Electrochemical frequency modulation (EFM)tests

EFM is a non-destructive corrosion measurement tests which can mark the corrosion current without prior information of Tafel slopes [69]. The EFM diagrams for Ranitidine in 1M HCl solution at 298 K with and without various concentration of Ranitidine had displayed in Fig. 10. The EFM parameters such as (CF-2 and CF-3), (β_c and β_a) and (i_{corr}) can be measured from the higher current peaks. The CF is closer to the standard data demonstrated the validity of the calculated data [70-71]. The IE_{EFM} % improve by raising the studied Ranitidine concentrations and was measured as next

$$\%IE_{EFM} = [1-(i_{corr}/i^{o}_{corr})] \times 100 \quad (11)$$

where i_{corr} and i^{o}_{corr} are corrosion current in the presence and absence of Ranitidine, respectively

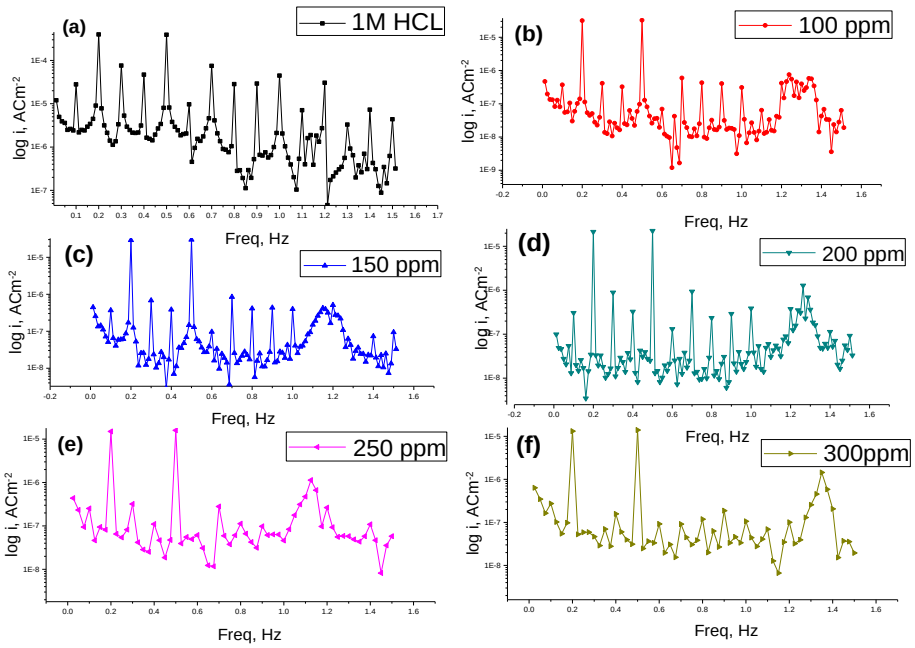

Figure 10 (a-f). EFM spectra for α-brass corrosion in the presence and absence of various concentrations of Ranitidine at 25˚C

Table 7. EFM data for Ranitidine in1 M HCl solutions containing various concentrations of the Ranitidine at 25°C

Conc, ppm	**i_{corr}, µA**	**β_a mV dec^{-1}**	**β_c mV dec^{-1}**	**CR. mpy**	**CF-2**	**CF-3**	**θ**	**% IE**
Blank	256.3	36	64	124	1.7	2.8	0.776	77.6
100	57.3	97	107	27	1.6	2.9	0.841	84.1
150	40.7	89	104	19	1.9	3.0	0.847	84.7
200	39.1	88	115	19	2.5	3.2	0.860	86.0
250	35.8	100	114	17	2.2	3.1	0.883	88.3
300	29.9	101	104	14	2.3	3.2	0.891	89.1

3.8. AFM Analyses

AFM is a dynamic tool to inspect the surface morphology from nano to microscale. AFM is a remarkable test utilized for measuring the surface roughness with high resolution [72]. AFM examination help to explain the corrosion process. The three-dimensional AFM shown in Fig. (11).

Table 8. AFM data for brass surface with and without inhibitor environment.

Sample	Average roughness (**Sa**) nm
Free	15
Blank	302
ER inhibitor	49

The roughness calculated from AFM image are summarize in Table (8). The outcome data displayed that the roughness increases with HCl addition due to the corrosion happens on the alpha brass surface but lowered with existence the Ranitidine

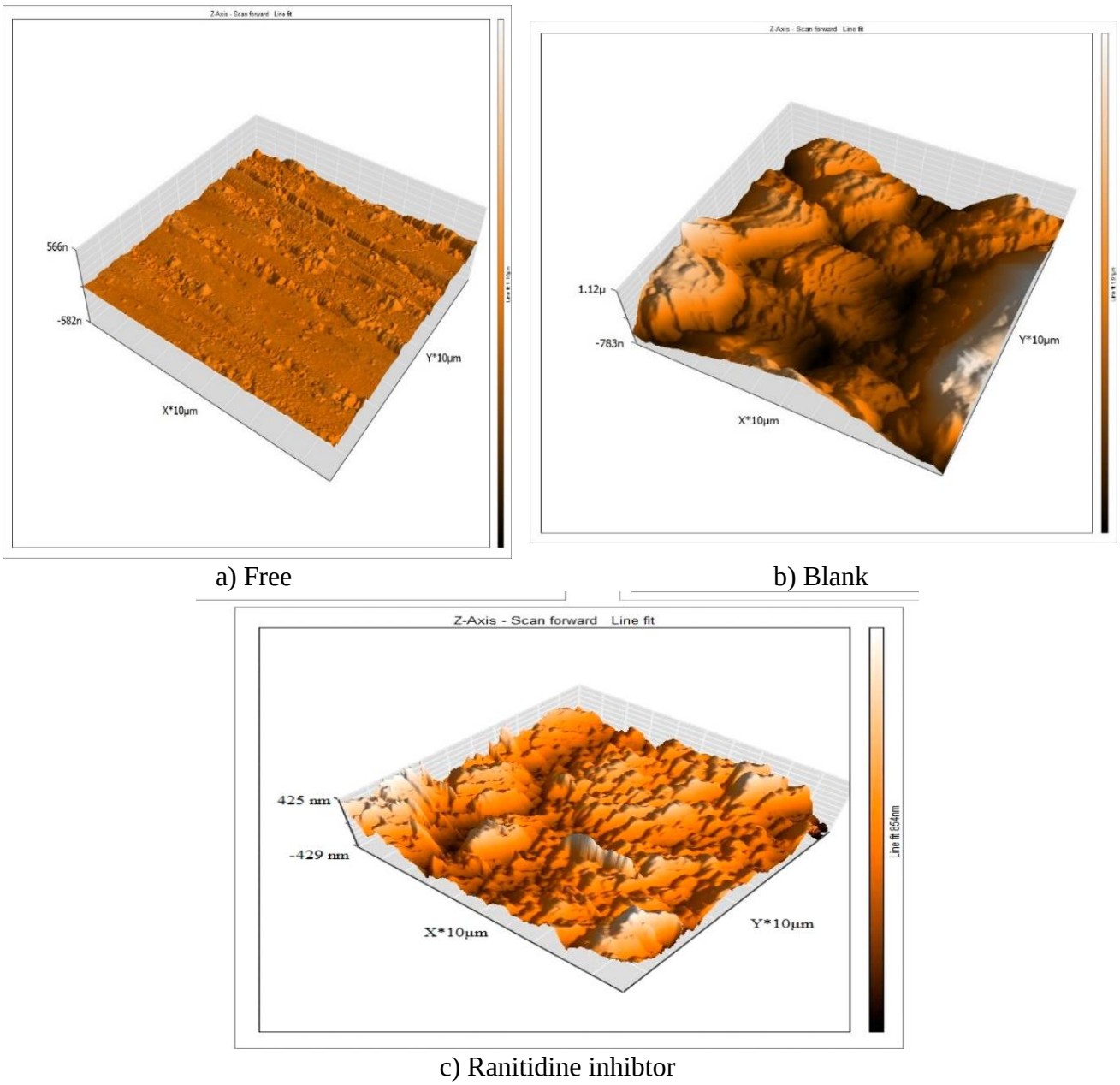

a) Free b) Blank

c) Ranitidine inhibtor

Figure 11. AFM 3D images alpha brass, free specimen, with 1M HCl for 24 hours with and without containing Ranitidine

3.9. SEM test

Figure 12 display the micrograph given for α-brass sheets in absence and using 300 ppm of Ranitidine after dipping for only one day. From SEM image, the α-brass surface is more degradation due to corrosion attack in HCl. The Ranitidine adsorption on the α-brass surface, forming the protective layer resulting in blocking the surface-active areas so that the α-brass become smoother and protection.

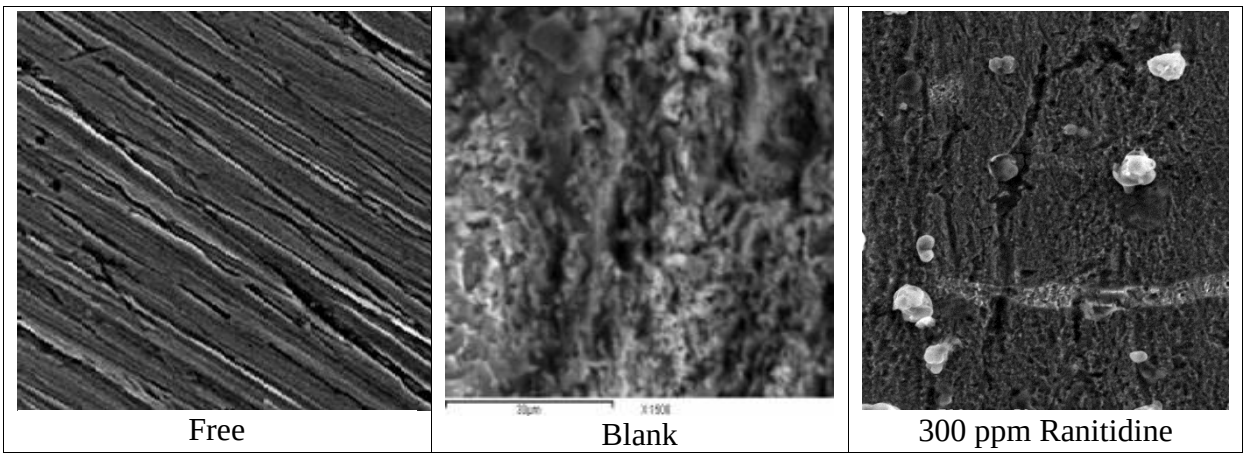

Figure 12. SEM image for brass with and without 300 ppm of Ranitidine after immersion for 24 hours at 25°C

3.10. Energy Dispersion Spectroscopy (EDX) Studies

Figure 13.a demonstrations the EDX data on the composition of α-brass with and without existence of Ranitidine. The EDX designates that only Fe and O were noticed, which shows that the passive film confined only Fe_2O_3. Fig. (13.b) Portray of the EDX investigation of α-brass in 1 M HCl only and Fig. (13c) shows the EDX of brass in the existence of 300 ppm of Ranitidine. The spectra demonstration added lines, representative the attendance of Cu (owing to the Cu atoms of Ranitidine). These outcome data demonstrations that the Cu and Zn materials protected the α- brass.

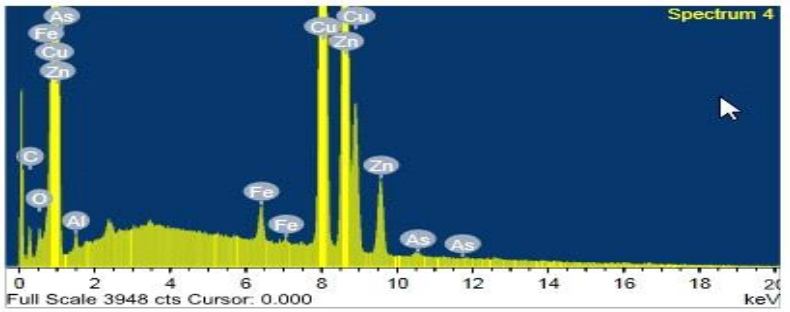

(a)

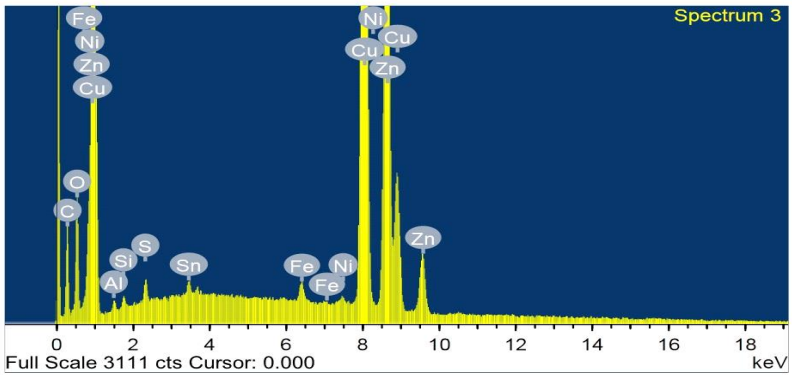

(b)

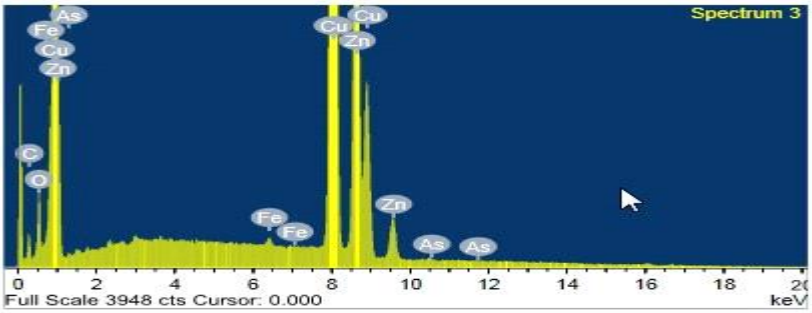

(c)

Figure 13. (a) EDX on Brass (free) (13b) Blank of α-brass in1M HCl (13c) brass in 1M HCl with the presence of ER.

Table 9. Weight % of α-brass after 24h of immersion in HCl without and with the 300 ppm Ranitidine

(% Mass)	**Cu**	**Zn**	**Fe**	**C**	**O**
Free	60.78	32.72	0.79	3.48	1.13
Blank	54.57	25.78	0.78	10.41	7.85
ER	38.10	20.21	--	28.82	12.53

3.11. (FT – IR) analysis

FTIR were achieved to check the adsorption of Ranitidine on α-brass.The FT-IR can be utilized to analyze the surface changes to prove the nature of the chemical components, which adsorbed on the α-brass.The peak at 3324 cm^{-1} is agreeing to the stretching of the amino group. This peak modified to 3355 cm^{-1} in the spectrum of the sample collected from the α-brass. Several peaks of Ranitidine in Fig. (14) are modified / disappeared designates the existence of bonds among nitrogen and oxygen atoms of the Ranitidine to the α-brass and agree the existence of adsorbed Ranitidine film on the brass surface [73].

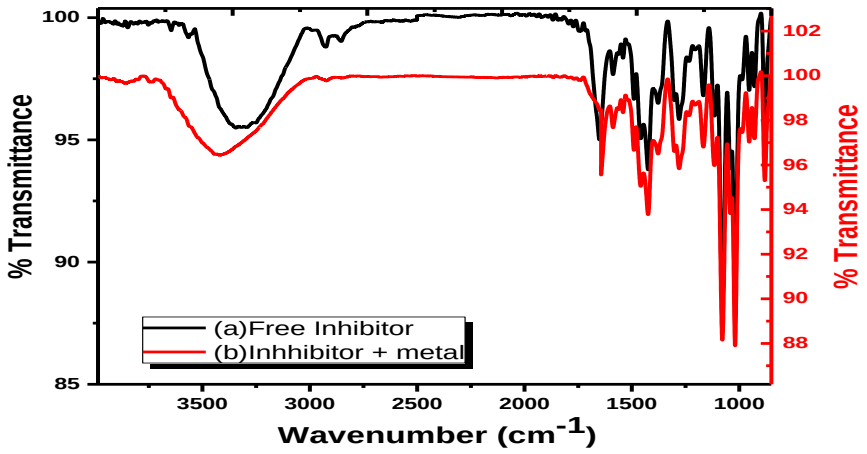

Figure 14. FT-IR spectra of Ranitidine (black spectrum line) and shielding film of Ranitidine on α-brass surface (the red spectrum line)

3.12. Quantum Chemical Calculations

The energy of frontier molecular orbitals can be associated with the reactivity of compounds and the corrosion inhibitive power of inhibitors [74]. The calculated quantum chemical parameters given in Table (10) such as LUMO and HOMO forms (E_{HOMO} and E_{LUMO}) and energy gap ΔE are the output of the DFT calculations. Generally, the inhibitor's active power is always associated with E_{HOMO} and E_{LUMO} [75]. Higher adsorption can be indicating from the higher value of E_{HOMO}, which means higher capacity of inhibitors to donate electrons in certain chemical interaction. Whereas, the low values of E_{LUMO} is indicative of the higher affinity of the inhibitor to accept electrons under some chemical interaction conditions. The gap energy ($\Delta E = E_{LUMO} - E_{HOMO}$), the lesser ΔE, the easier the electron transfer from HOMO to LUMO and the higher adsorption ability of the Ranitidine on brass, hence the IE will be greater. All outcome data in Table (10) displayed that the Ranitidine has the lowest total energy which means that the adsorption of the Ranitidine is higher Fig. (15) provides the electron density maps of HOMO and LUMO for the tested inhibitors.

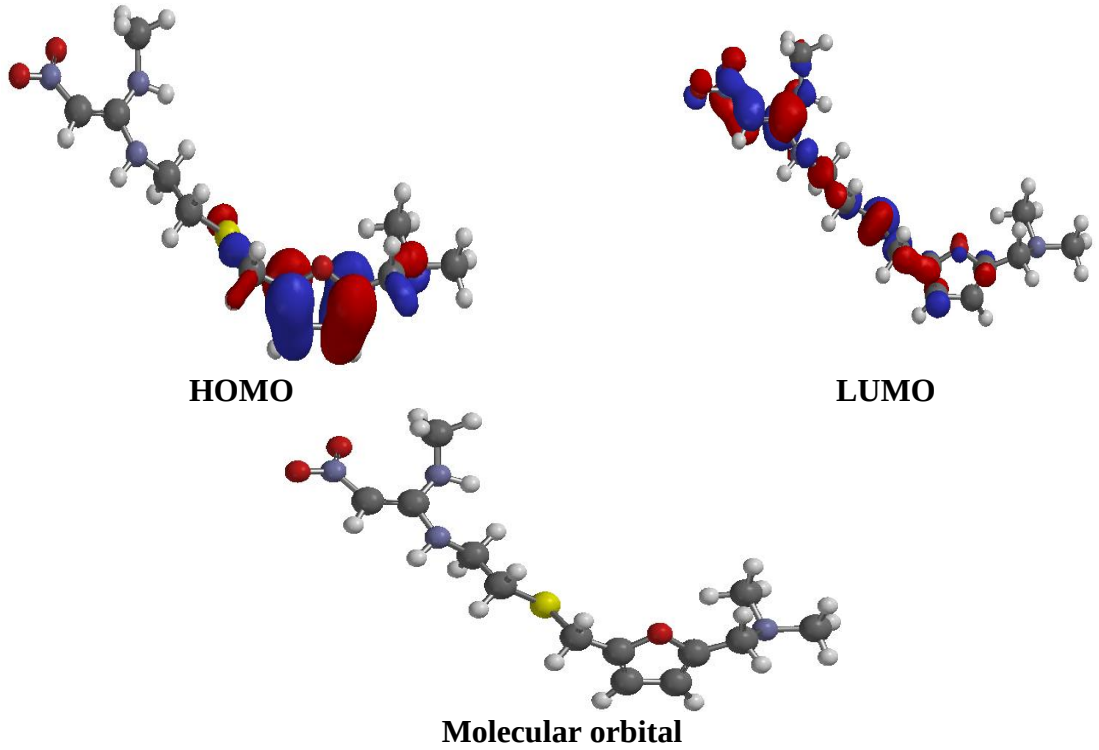

Figure 15. (HOMO) and (LUMO) of molecular orbital

Table 10. Calculated quantum chemical properties for the Ranitidine

E_{HOMO}, (ev)	**-9.27**
E_{LUMO}, (ev)	**-0.73**
ΔE, (E_L-E_H)	**8.540**
μ, (Dipole moment)	**8.140**

3.13. Inhibition Mechanism

Adsorption behavior of Ranitidine molecules depends on their physicochemical characteristics (e.g. types of electron density and functional groups) and the charge of α-brass. The possible inhibition process of Ranitidine on the surface of α-brass is explained on the bases of the results of the experimental analysis and theoretical calculations. A variety of research reported that the α-brass surface in HCl solution is positively charged, i.e., there are excess positive charges on the α-brass [76-77]. The α-brass surface with its positive charge prefers the adsorption of Cl^- ions to produce a negative charge surface, which enables the adsorption of the cations in the medium. Due to the unshared electron pair of the N and O electrons, Ranitidine can be protonated in the medium. The protonated molecules could adsorb on specimen of α-brass surface forming physical adsorption.

4. CONCLUSIONS

- Results gotten from the experimental display that Ranitidine excellent for the corrosion of α-brass.
- The %IE lowered with rise in temperature, prominent to the conclusion that the formed protective film on α-brass surface is less stable at higher temperature.
- The PP curves suggest that Ranitidine acts as a mixed kind inhibitor
- The adsorption obeys Langmuir isotherm.
- The polarization resistance (R_p) data improved with rise in the concentration of the Ranitidine
- The obtained data obtained from PP, EIS, EFM and ML tests are in good agreement with each other.

References

1. E. Stupnisek-Lisac, A. Loncaric Bozic and I. Cafuk, *Corrosion*, 54 (1998) 713.
2. R. Gasparac, C.R. Martin and E. Stupnisek-Lisac, *J. Electrochem. Soc*., 147 (2000) 548.
3. A.M. Zaky*, Br. Corros. J*., 36 (2001) 59.
4. R.F. North and M.J. Pryar, *Corros. Sci*., 10 (1970) 297.
5. M.A. Elmorsi, M.Y. El-Sheikh, A.M. Bastwesy and M.M. Ghoneim, *Bull. Electrochem*., 7 (1991) 158.
6. M.M. Osman, *Mater. Chem. Phys*., 71 (2001) 12.
7. M.A. Quraishi, I.H. Farooqi and P.A. Saini*, Br. Corros. J.*, 35 (2000) 78.
8. H.C. Shih and R.J. Tzou, *J. Electrochem. Soc*., 138 (1991) 958.
9. G. Quartarone, G. Moretti and T. Bellami, *Corrosion*, 54 (1998) 606.
10. A.G. Gad-Allah, M.M. Abou-Romia, M.W. Badawy and H.H. Rehan, *J. Appl. Electrochem*., 21 (1991) 829.
11. 11 Mitra, A.K., *R&D J. NTPC*, 2 (1996) 52.
12. D. Tianbao, C. Jiajian, C. Dianzhen, *J. Mater. Sci.,* 36 (2001) 3903.
13. P. Morales-Gil, G. Negron-Silva, M. Romero-Romo, C. Angeles-Chavez, M. Palomar- Pardave, *Electrochim. Acta.,* 49 (2004) 4733.

14. J. M. Bastidas, J. L. Polo, E. Cano, *J. Appl. Electrochem.*, 30 (2000) 1173.
15. B. Zerga, A. Attiyibat, M. Sfaira, M. Taleb, B. Hammouti, M. Ebn Touhami, S. Radi, Z. Rais, *J. Appl. Electrochem.,* 40 (2010**)** 1575.
16. S. Tamil Selvi, V. Raman, N. Rajendran, *J. Appl. Electrochem.,* 33 (2003) 1175.
17. P. Lowmunkhong, D. Ungthararak, P. Sutthivaiyakit, *Corros. Sci.,* 52 (2009) 30.
18. M. Zerfaoui, H. Oujda, B. Hammouti, S. Kertit, M. Benkaddour, *Prog. Org. Coat.,* 51 (2004) 134.
19. A. Chetaouani, B. Hammouti, A. Aouniti, N. Benchat, T. Benhadda, *Prog. Org. Coat.*, 45 (2002) 373.
20. K. A. Mohamed, *J. Electroanal. Chem.,* 567 (2004) 219.
21. D. K. Yadav, B. Maiti, M. A. Quraishi, *Corros. Sci.,* 52 (2010) 3586.
22. K. S. Jacob, G. Parameswaran, *Corros. Sci.*, 52 (2009) 224.
23. A. Ostovari, S. M. Hoseinieh, M. Peikari, S. R. Shadizadeh, S. J. Hashemi, *Corros. Sci.*, 51(2009) 1935.
24. A. S. Fouda, S. A. Abd El-Maksoud, A. El-Hossiany, A. Ibrahim, *Int. J. Electrochem. Sci.,* 14 (2019) 6045.
25. A.K. Satapathy, G. Gunasekaran, S.C. Sahoo, K. Amit, P.V. Rodrigues, *Corros. Sci*., 51 (2009**)** 2848.
26. X. H. Li, S. D. Deng, H. Fu, *J. Appl. Electrochem*., 40 (2010) 1641.
27. A. S Fouda, A.M. El-Wakeel, K. Shalabi and A. El-Hossiany, *Elixir Corrosion & Dye*, 83 (2015) 33086.
28. R. S. Abd El Hameed, H. I. Al Shafey, S. A. Soliman, M. S. Metwally, *Al Azhar Bull. Sci.,* 19 (2008) 283.
29. F.C. Giacomelli, C. Giacomelli, M.F. Amadori, V. Schmidt, A. Spinelli, *Mater. Chem. Phys.,* 83 (2004) 124
30. R. S. Abd El Hameed, H. I. Al Shafey, E. A. Ismail, *Al Azhar Bull. Sci.,* 20 (2009) 185.
31. A. S. Fouda, K. Shalabi, A. El-Hossiany, *J. Bio. Tribo. Corros*., 2 (2016) 18.
32. I. B. Obot, N.O. Obi-Egbedi, S.A. Umoren, *Corros. Sci.,* 51 (2009) 1868.
33. M. Abdallah, *Corros. Sci*., 46 (2004) 1981.
34. A. S Fouda, A. El-Hossiany, H. Ramadan, *int. J. Appl. Eng. Res*., 5(2017)1698.
35. I.B. Obot, N.O. Obi-Egbedi, *E-J. Chem*., 7 (2010) 837.
36. R. S. A. Hameed, *Al Azhar Bull. Sci*., 20 (2009) 151.
37. A. S Fouda, A. El-Hossiany, H. Ramadan, *Zastita Materijala*, 58(4) (2017)541.
38. K. F. Khaled, *Mater. Chem. Phys.,* 112 (2008) 290.
39. K. F. Khaled, *J. Appl. Electrochem*., 39 (2009) 429.
40. R. W. Bosch, J. Hubrecht, W. F. Bogaerts, B. C. Syrett, *Corrosion,* 57 (2001) 60.
41. S. S. Abdel–Rehim, K. F. Khaled, N. S. Abd–Elshafi, *Electrochim. Acta*, 51 (2006) 3269
42. A.S. Fouda, S. Rashwan, A. El-Hossiany, F. E. El-Morsy, *J. Chem. Bio. Phy. Sci. Sec. A,* 9(1)(2019)1.
43. M. M. Saleh, A. A. Atia, *J. Appl. Electrochem*., 36 (2006) 899.
44. Narvaez, L., Cano, E., and Bastidas, D.M., *J. Appl*. *Electrochem*., 35 (2005) 499.
45. X. H. Li, S. D. Deng, H. Fu, *Corros. Sci*., 51 (2009) 1344.
46. E. Cano, J. L. Polo, A. La Iglesia, J. M. Bastidas, *Adsorption*, 10 (2004) 219.
47. A.S. Fouda, M. Eissa, A. El-Hossiany, *Int. J. Electrochem. Sci.,* 13 (2018) 11096.
48. A. Yurt, G. Bereket, A. Kivrak, A. Balaban, B. Erk, *J. Appl. Electrochem.*, 35 (2005) 1025.
49. F. Bentiss, M. Traisnel, M. Lagrenee, *Corros Sci.,* 42 (2000) 127.
50. F. Bentiss, M. Lebrini, M. Lagrenee, *Corros. Sci.,* 47 (2005) 2915.
51. Y. Ait Albrimi, A. Ait Addi, J. Douch, R. M. Souto, M. Hamdani, *Corros. Sci.*, 90(2015)522
52. A.S. Fouda, S. A. Abd El-Maksoud, A. M. Belal, A. El-Hossiany, A. Ibrahim*, Int. J. Electrochem. Sci*., 13 (2018) 9826.
53. Z. H. Tao, S. T. Zhang, W. H. Li, B. R. Hou, *Corros. Sci*., 51 (2009) 2588.

54. E. S. Ferreira, C. Giacomelli, F. Giacomelli, A. Spinelli, *Mater. Chem. Phys*., 83 (2004) 129.
55. D. C. Silverman, J. E. Carrico, *Corrosion,* 44(1988) 280.
56. W. J. Lorenz, F. Mansfeld, *Corros. Sci.,* 21 (1981) 647.
57. D. D. Macdonald, M. C. Mckubre, *Modern Aspects of Electrochem., J. O'M. Bockris, B.E. Conway, R.E. White, Eds., Plenum Press, New York,* 14(1982)61.
58. F. Mansfeld, *Corrosion,* 36(1981) 301.
59. M. M. Motawe, A.El-Hossiany, A. S. Fouda, *Int. J. Electrochem. Sci.,* 14(2019)1372.
60. M. El Achouri, S. Kertit, H. M. Gouttaya, B. Nciri, Y. Bensouda, L. Perez, M. R. Infante, K. Elkacemi, *Prog. Org. Coat.,* 43 (2001) 267.
61. *R.S. Abdel Hameed / Port. Electrochim. Acta,* 29 (2011) 273.
62. S. F. Mertens, C. Xhoffer, B. C. Decooman, E. Temmerman, *Corrosion,* 53 (1997) 381.
63. G. Trabanelli, C. Montecelli, V. Grassi, A. Frignani, *J. Cem. Concr., Res.,* 35 (2005) 1804.
64. A. S. Fouda, M. Abdel Azeem, S.A.Mohamed, A.El-Hossiany and E. El-Desouky, *Int. J. Electrochem. Sci.,* 14 (2019) 3932.
65. F. M. Reis, H.G. De Melo, I. Costa, *Electrochim. Acta,* 51 (2006) 17.
66. M. Lagrenee, B. Mernari, M. Bouanis, M. Traisnel, F. Bentiss, *Corros. Sci.,* 44 (2002) 573.
67. E. M. Cafferty, N. Hackerman, *J. Electrochem. Soc.,* 119 (1972) 146.
68. H. Ma, S. Chen, L. Niu, S. Zhao, S. Li, D. Li, *J. Appl. Electrochem.,* 32 (2002) 65.
69. E. Kus, F. Mansfeld, *Corros. Sci.,* 48 (2006) 965.
70. G. A. Caigman, S. K. Metcalf, E. M. Holt, *J. Chem. Cryst.,* 30 (2000) 415.
71. S. S. Abdel–Rahim, K. F. Khaled, N. S. Abd–Elshafi, *Electrochim. Acta,* 51 (2006) 3269.
72. A. S. Fouda, S. A. Abd El-Maksoud, A. El-Hossiany, A. Ibrahim, *Int. J. Electrochem. Sci*., 14 (2019) 2187.
73. A.S. Fouda, Ibrahim, Rashawn, A. El-Hossiany, R.M. Ahmed*, Int. J. Electrochem. Sci.,* 13 (2018) 6327
74. L. Jiang, Y. Qiang, Z. Lei, J. Wang, Z. Qin, B. Xiang, *J. Mol. Liq.,* 255 (2018) 53.
75. K. Alaoui, M. Ouakki, A.S. Abousalem, H. Serrar, M. Galai, S. Derbali, K. Nouneh, S. Boukhris, M. E. Touhami, Y. El Kacimi, *J. Bio- Tribo-Corrosion,* 5 (2019) 1
76. S. Deng, X. Li, X. Xie, *Corros. Sci.,* 80 (2014) 276.
77. R. M. Issa, M. K. Awad, F. M. Atlam, *Appl. Surf. Sci.,* 255 (2008) 2433.